Chapter 2

Quantifying the performance of a new T cell sorting technique, and the preparation of reagents for quantitative analysis of proteins from macrophages

2.1. Introduction

In this chapter, I will briefly present the background of two projects in which I took participation at the early years of my graduate studies and give explanations about my contribution on each projects: the quantification of a novel sorting method for tumor antigen specific T cells and the preparation of reagents for the quantitative analysis of protein signaling network in macrophages.

T cells, which play a central role in an adaptive immune response, recognize different antigens via the interaction between T cell receptor (TCR) and antigenic peptides bound to Major Histocompatibility Complex (p/MHC) on the surface of antigen presenting cells (APC). In order to detect antigen-specific T cells, four enzymatically biotinylated p/MHC monomers are coupled with a streptavidin molecule primed by chromophore to form a p/MHC tetramer, and the tetramer enables its counter part T cell to be detected via flow cytometry[1].

The p/MHC tetramer based flow cytometry has inevitable restrictions. At first, each antigen-specificity requires unique optical dye molecule having little spectral overlap with others. Secondly, the existence of detection limit in flow cytometry, serial

flow cytometry detection for multiplexing study is restricted by the sample size. Due to the existence of diverse optical characters in each cell population, moreover, the matter of compensation always follows. Although researchers used polychromatic flow cytometry utilizing quantum dots to resolve those problems[2-4], high cost, long sample preparation time, and complex color compensation still hinder further study.

To avoid such problems, several researchers have reported antigen-specific cell sorting by microarrays, which is contains directly printed p/MHC tetramers on a supporting substrates[5-8]. When a population of cells is applied on the array, only target antigen-specific T cells bind to the region having p/MHC tetramers. Because this method uses the location of p/MHC tetramers to separate a target antigen-specific T cell from the variety of other cells instead of the chromophore's emission spectrum, multiplexing is only restricted the number of reagent able to fit on a substrate.

In order to increase the capture efficiency, orientation of p/MHC tetramer should be preserved in a way to react approaching cells and the tetramer must not be denatured through the microarray fabrication. Analogous protein arrays, made via antibody adsorption to unmodified and derivatized surfaces, have shown that the adsorbed antibodies could fully react because of surface-induced effects such as protein denaturation and orientational change to inactive. As the result, amount of functional antibody is decreased, immobilization occurs heterogeneously, and required concentrations of antibody is increased to compensate for the protein loss[9-11]. To avoid these problems, several mild chemistries have been studied for protein immobilization[12-18], but often the surface that meets the demands of application requires a high level of

technical expertise and/or is limited in accessibility. Therefore, the development of a new technology to fabricate p/MHC array in an easy way is important.

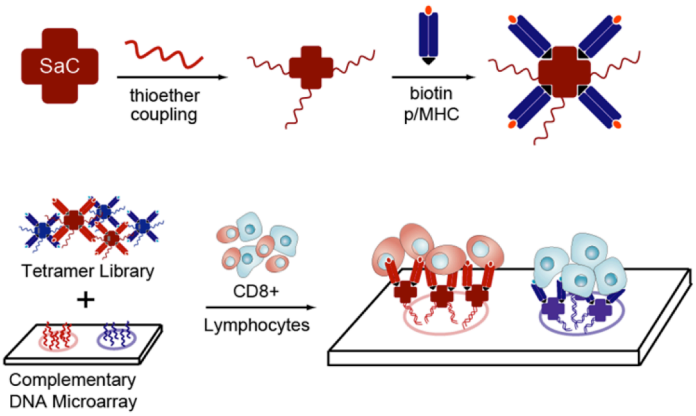

Fig. 2.1. Self-assembled ssDNA-p/MHC tetramer arrays for multiplexed sorting of antigen-specific cells. ssDNA-encoded p/MHC tetramers are produced by coupling ssDNA site-specifically to SAC prior to exposure to molar excess of biotinylated p/MHC monomers. p/MHC tetramer arrays are formed by pooling ssDNA-p/MHC tetramers of select specificity and hybridization to a complementary printed ssDNA microarray. T cells expressing the cognate TCR are detected by binding to the surface confined tetramer.

In Heath lab, a new p/MHC arrays conjugated with nucleic acid for multiplexed antigen-specific lymphocytes sorting is developed. Instead of direct printing, each specific p/MHC tetramer is conjugated to unique sequence of ssDNA designed to be orthogonal to other sequences. On the glass surface where the complementary DNA sequences are printed, the ssDNA-p/MHC tetramer conjugates are self-assembled by DNA hybridization, then used as a p/MHC array to sort mixed population of antigen-specific T cells (**Fig. 2.1.**). This method is called "Nucleic Acid Cell Sorting (NACS)." Because NACS employs DNA as a linkage molecule, fabrication of p/MHC arrays is simple and highly modular[19-22]. Traditional DNA microarray technologies are also available to make cDNA glass substrates. In order to produce ssDNA-p/MHC tetramer

conjugates having maximum capacity to immobilize cells, cysteine-engineered SA (SAC) is used a scaffold. NACS arrays have better performance than traditional p/MHC arrays made by direct printing, and the specificity, multiplexing and sensitivity of NACS are studied. Selective detachment after sell sorting by NACS and its application to primary human T cells is also introduced. The detailed results are shown in Appendix A, as well as in *J. Am. Chem. Soc.*, **2009**, *131*(28), 9695–9703.

Protein-signaling pathways play important roles in tissue processes ranging from tumorigenesis to wound healing. Elucidation of these signaling pathways is challenging, in large part[23-27], because of the heterogeneous nature of tissues[4]. Such heterogeneity makes it difficult to separate cell-autonomous alterations in function from alterations that are triggered via paracrine signaling, and it can mask the cellular origins of paracrine signaling. Intracellular signaling pathways can be resolved via multiplex protein measurements at the single-cell level[28]. For secreted protein signaling, there are additional experimental challenges. Intracellular staining flow cytometry (ICS-FC) requires the use of protein transport inhibitors which can influence the measurements[3]. In addition, the largest number of cytokines simultaneously assayed in single-cells by ICS-FC is only 5^2. Finally, certain biological perturbations, such as the influence of one cell on another, are difficult to decipher using ICS-FC. Other methods, such as multiplex fluorospot assays[23-27,29], have even more significant limitations.

In Heath lab, an experimental/theoretical approach designed to unravel the coordinated relationships between secreted proteins, and to understand how molecular and cellular perturbations can influence those relationships. The starting points are single,

lipopolysaccharide (LPS)-stimulated, human macrophage cells[4,30]. LPS stimulation activates the Toll-like Receptor-4 (TLR-4), and emulates the innate immune response to Gram-negative bacteria. We characterize the secretome, at the single-cell level, through the use of a microchip platform in which single, stimulated macrophage cells are isolated into 3 nanoliter (nl) volume microchambers, with ~1000 microchambers per chip. Each microchamber permits duplicate assays for each of a dozen proteins that are secreted over the course of a several-hour incubation period following cell stimulation. The barcode assays are developed using detection antibodies and fluorescent labels, and then converted into numbers of molecules detected (**Fig. 2.2.**). We demonstrate that the observed spread in protein levels is dominated by the cellular behaviors (the biological fluctuations), rather than the experimental error. These fluctuations are utilized to compute a covariance matrix linking the different proteins. This matrix is analyzed at both coarse and fine levels to extract the protein-protein interactions. We demonstrate that our system has the stability properties requisite for the application of a quantitative version of a Le Chatelier-like principle, which permits a description of the response of the system to a perturbation. This is a prediction in the strict thermodynamic sense. The fluctuations, as assessed from the multiplexed protein assays from unperturbed single-cells, are used to predict the results when the cells are perturbed by the presence of other cells, or through molecular (antibody) perturbations. The detailed results are shown in Appendix B, as well as in *Biophys. J.,* **2011**, *100(10),* 2378-2386.

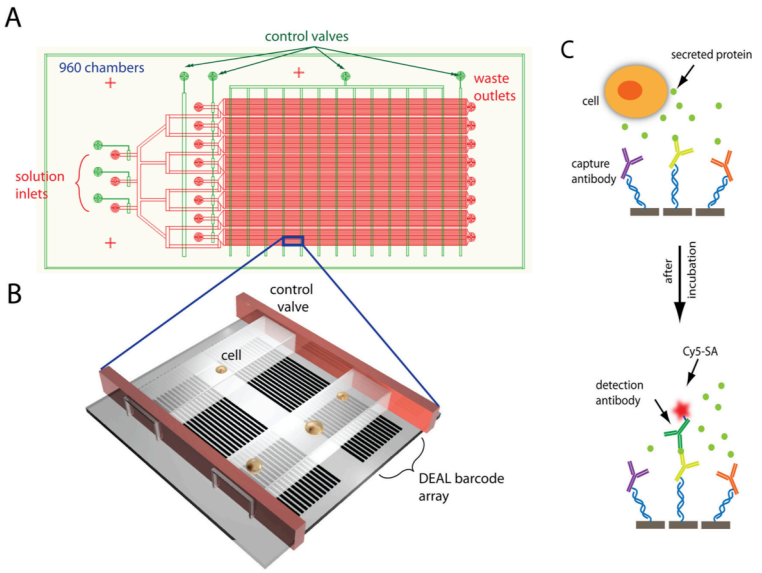

Fig. 2.2. Design of integrated microchip for single-cell protein secretome analysis. (A) CAD design of a microchip in which flow channels are shown in red and the control channels are shown in green. (B) Schematic drawing of cells loaded in the microchambers and compartmentalized with the valves pressurized. (C) Schematic illustration of the antibody barcode array used for multiplexed immunoassay of single-cell secreted proteins.

2.2. Experimental Methods

2.2.1. Microarray fabrication for T cell sorting

All DNAs were acquired from IDT. By the facility at the Institute for Systems Biology (ISB, Seattle), DNA strands were printed on amine coated glass slides (GAPSII, Corning) in the way to form 12x12 arrays having alternative rows of A, B, and C spots with a SMPXB15 pin (Arrayit). Sequence of each strand and its counterparts is written at the following **Table 2.1.**

Table 2.1. Orthogonal DNA sequences for spatial encoding of p/MHC tetramers

Name	Sequence*
A	5' - AAA AAA AAA AAA AAT CCT GGA GCT AAG TCC GTA AAA AAA AAA AAT CCT GGA GCT AAG TCC GTA AAA AAA AAA AAA A
A'	5' - NH_2- AAA AAA AAA ATA CGG ACT TAG CTC CAG GAT
B	5' - AAA AAA AAA AAA AGC CTC ATT GAA TCA TGC CTA AAA AAA AAA AGC CTC ATT GAA TCA TGC CTA AAA AAA AAA AAA A
B'	5' - NH_2- AAA AAA AAA ATA GGC ATG ATT CAA TGA GGC
C	5' - AAA AAA AAA AAA AGC ACT CGT CTA CTA TCG CTA AAA AAA AAA AGC ACT CGT CTA CTA TCG CTA AAA AAA AAA AAA A
C'	5' - NH_2- AAA AAA AAA ATA GCG ATA GTA GAC GAG TGC

* All sequences to be conjugated to SAC (A', B', C') were designed with a polyA linker followed by a 20mer hybridization region. The 5' amine is required for the attachment of the hetero-bifunctional maleimide derivative MHPH. Sequences printed on glass substrates (A, B, C) were designed with two hybridization regions separated by polyAs. This was designed to facilitate electrostatic adsorption to amine glass substrates.

2.2.2. Synthesis of DNA-SAC conjugates

In order to express SAC, pET-3a plasmid, as a kind gift from Takeshi Sano (Harvard Medical School), was used. SAC was expressed according to the previously published protocol[31], and buffer exchanged to PBS with 5 mM Tris(2-carboxyethyl) phosphine hydrochloride (Solulink), using zeba desalting columns (Pierce). MHPH (3-N-Maleimido-6-hydraziniumpyridine hydrochloride, Solulink) was added to SAC at a molar excess of 300:1. Meanwhile, SFB (Succinimidyl 4-formylbenzamide, Solulink) in DMF was added to 5' aminated DNA oligos at a molar excess of 40:1. In order to finish reactions, these mixtures were incubated at room temperature (RT) for 3-4 hours. Then,

both mixture were buffer exchanged to pH 6.0 buffer solution (50 mM sodium citrate, 150 mM NaCl), and SFB-conjugated DNA oligos were added to MHPH-conjugated SAC at a molar excess of 20:1, and incubated overnight at RT. With Phamacia Superdex 200 gel filtration column at 0.5 ml/min isocratic flow of PBS, SAC-DNA oligo conjugates was purified, and concentrated by 10K mwco concentration filters (Millipore).

2.2.3. Preparation of T cells

In order to make Jurkat$^{a\text{-}MART\text{-}1}$ cells, MSGV1-F5AfT2AB retroviral vector expressing the F5 MART-1 TCR, obtained from Steven A. Rosenberg and Richard Morgan (Surgery Branch, National Cancer Institute Bethesda, MD), was used to infect Jurkat cells. Cells were culture with RPMI 1640 (ATCC) supplemented with 10% Fetal Bovine Serum (ATCC).

2.2.4. Sorting cells with NACS and conventional microarrays

The HLA-A*0201 restricted MHC class I monomers loaded with MART-126-35 (ELAGIGILTV) were made in house with previous published protocols[32], and lipophilic cell membrane staining dyes DiO, DiD, and DiL were obtained from Invitrogen.

To prevent non-specific cell binding, 1mg/ml PEG-NHS ester (Sunbio) in PBS was applied on microarray slides for 2 hours at RT. p/MHC monomers were combined in a 4:1 molar excess with ssDNA-SAC at 37^{o}C for 20 min to form ssDNA-p/MHC tetramers. With the tetramers in 200µl media, DNA microarrays was hybridized for 1 hour at 37^{o}C, and washed with 3% FBS in PBS. T cells (10^6 cells/ml) were incubated on the array for 30 min at 37^{o}C, and washed with the same media.

To compare the performance of sorting with conventional microarray techniques, SuperEpoxy(covalent) and SuperProtein(hydrophobic) slides were obtained from Arrayit, GAPSII(electrostatic) slide was purchased from Corning, and Hydrogel(hydrophilic) slide was acquired from Xantec. According to manufacturer's protocol, fluorescent MART-1 tetramers were immobilized on each slide, and the result was analyzed with ImageJ and Origin. All cell capture images were obtained by bright filed (Nikon Eclipse TE2000) and/or confocal microscopy (Nikon E800).

2.2.5. Microchip fabrication.

The Single-cell barcode chips (SCBC) were assembled from a DNA barcode microarray glass slide and a PDMS slab containing a microfluidic circuit[22,33]. The DNA barcode array was created with microchannel-guided flow patterning technique[33]. Each barcode was comprised of thirteen stripes of uniquely designed ssDNA molecules. PDMS microfluidic chip was fabricated using a two-layer soft lithography approach[34]. The control layer was molded from a SU8 2010 negative photoresist (~ 20 μm in thickness) silicon master using a mixture of GE RTV 615 PDMS prepolymer part A and part B (5:1). The flow layer was fabricated by spin-casting the pre-polymer of GE RTV 615 PDMS part A and part B (20:1) onto a SPR 220 positive photoresist master at ~2000 rpm for 1minute. The SPR 220 mold was ~ 18 mm in height after rounding via thermal treatment. The control layer PDMS chip was then carefully aligned and placed onto the flow layer, which was still situated on its silicon master mold, and an additional 60 min thermal treatment at 80 °C was performed to enable bonding. Afterward, this two-layer PDMS chip was cut off and access holes drilled. In order to improve the biocompatibility of PDMS, we performed

a solvent extraction step, which removes uncrosslinked oligomers, solvent and residues of the curing agent through serial extractions/washes of PDMS with several solvents[35,36]. We noticed that this step significantly improves the biocompatibility and the reproducible protein detection. Finally, the microfluidic-containing PDMS slab was thermally bonded onto the barcode-patterned glass slide to give a fully assembled microchip.

2.2.6. Preparation of barcode arrays

The barcode array initially consists of 13 uniquely designed DNA strands labeled in order as A through M. Prior to loading cells, a cocktail containing all capture antibodies conjugated to different complementary DNA strands (A'-L') is flowed through the chambers, thus transforming, via DNA hybridization, the DNA barcode into an antibody array. These dozen proteins that comprised the panel used here were encoded by the DNA strands A through L, respectively. The DNA oligomer sequences and the antibody pairs used are listed in **Table 2.2.** and **Table 2.3.** DNA-encoded antibodies were synthesized as previously described[18] and quantified with BCA kit (Pierce) according to the manufacturer's guide.

Table 2.2. Sequences and terminal functionalization of oligonucleotides*.

Name	Sequence
A	5'- AAA AAA AAA AAA AGT CCT CGC TTC GTC TAT GAG-3'
A'	5' NH3-AAA AAA AAA ACT CAT AGA CGA AGC GAG GAC-3'
B	5'-AAA AAA AAA AAA AGC CTC ATT GAA TCA TGC CTA -3'
B'	5' NH3-AAA AAA AAA ATA GGC ATG ATT CAA TGA GGC -3'
C	5'- AAA AAA AAA AAA AGC ACT CGT CTA CTA TCG CTA -3'
C'	5' NH3-AAA AAA AAA ATA GCG ATA GTA GAC GAG TGC -3'
D	5'-AAA AAA AAA AAA AAT GGT CGA GAT GTC AGA GTA -3'
D'	5' NH3-AAA AAA AAA ATA CTC TGA CAT CTC GAC CAT -3'
E	5'-AAA AAA AAA AAA AAT GTG AAG TGG CAG TAT CTA -3'
E'	5' NH3-AAA AAA AAA ATA GAT ACT GCC ACT TCA CAT -3'
F	5'-AAA AAA AAA AAA AAT CAG GTA AGG TTC ACG GTA -3'
F'	5' NH3-AAA AAA AAA ATA CCG TGA ACC TTA CCT GAT -3'
G	5'-AAA AAA AAA AGA GTA GCC TTC CCG AGC ATT-3'
G'	5' NH3-AAA AAA AAA AAA TGC TCG GGA AGG CTA CTC-3'
H	5'-AAA AAA AAA AAT TGA CCA AAC TGC GGT GCG-3'
H'	5' NH3-AAA AAA AAA ACG CAC CGC AGT TTG GTC AAT-3'
I	5'-AAA AAA AAA ATG CCC TAT TGT TGC GTC GGA-3'
I'	5' NH3-AAA AAA AAA ATC CGA CGC AAC AAT AGG GCA-3'
J	5'-AAA AAA AAA ATC TTC TAG TTG TCG AGC AGG-3'
J'	5' NH3-AAA AAA AAA ACC TGC TCG ACA ACT AGA AGA-3'
K	5'-AAA AAA AAA ATA ATC TAA TTC TGG TCG CGG-3'
K'	5' NH3-AAA AAA AAA ACC GCG ACC AGA ATT AGA TTA-3'
L	5'-AAA AAA AAA AGT GAT TAA GTC TGC TTC GGC-3'
L'	5' NH3-AAA AAA AAA AGC CGA AGC AGA CTT AAT CAC-3'
M	5'-AAA AAA AAA AGT CGA GGA TTC TGA ACC TGT-3'
M'	5' Cy3-AAA AAA AAA AAC AGG TTC AGA ATC CTC GAC-3'

* All oligonucleotides were synthesized by Integrated DNA Technology (IDT) and purified via high-performance liquid chromatography (HPLC).

Table 2.3. Summary of antibodies used for macrophage experiments

DNA label	primary antibody (vendor)	secondary antibody (vendor)
A'	mouse anti-hu IL-2 (BD Biosciences)	biotin-labeled mouse anti-hu IL-2 (BD Biosciences)
B'	mouse anti-hu MCP-1 (eBioscience)	biotin-labeled armenian hamster anti-hu MCP-1 (eBioscience)
C'	rat anti-hu IL-6 (eBioscience)	biotin-labeled rat anti-hu IL-6 (eBioscience)
D'	rat anti-hu GMCSF (Biolegend)	biotin-labeled rat anti-hu GMCSF (Biolegend)
E'	goat anti-hu MIF(R&D systems)	biotin-labeled goat anti-hu MIF(R&D systems)
F'	mouse anti-hu IFN-γ (eBioscience)	biotin-labeled mouse anti-hu IFN-γ (eBioscience)
G'	mouse anti-hu VEGF (R&D systems)	biotin-labeled goat anti-hu VEGF (R&D systems)
H'	mouse anti-hu IL-1β (eBioscience)	biotin-labeled mouse anti-hu IL-1β (eBioscience)
I'	rat anti-hu IL-10 (eBioscience)	biotin-labeled rat anti-hu IL-10 (eBioscience)
J'	mouse anti-hu IL-8 (R&D systems)	biotin-labeled mouse anti-hu IL-8 (R&D systems)
K'	mouse anti-hu MMP9 (R&D systems)	biotin-labeled goat anti-hu MMP9 (R&D systems)
L'	mouse anti-hu TNF-α (eBioscience)	biotin-labeled mouse anti-hu TNF-α (eBioscience)

2.3. Results and Discussions

2.3.1. Comparison between NACS and conventional protein microarray

For the comparison study between NACS and conventional microarrays based on direct protein spotting method, I chose various substrates to cover different spectrum of commonly used strategies (covalent, electrostatic, hydrophobic, and hydrophilic adsorption) for protein immobilization. According to manufacturer's instruction, serial dilutions of MART-1 SA-PE tetramer (HLA-A2.1 MHC molecules loading melanoma epitope MART-1_{26-35}) were directly printed. Onto these microarray, Jurkat$^{a\text{-MART-1}}$ T cells (Jurkat cells transduced with the F5 MART-1 TCR[37] specific for peptide epitope MART-1_{26-35}) were applied. Collected images of immobilized cells on the various substrates (**Fig. 2.3.a**) and quantified analysis **(Fig. 2.3.b**) were obtained.

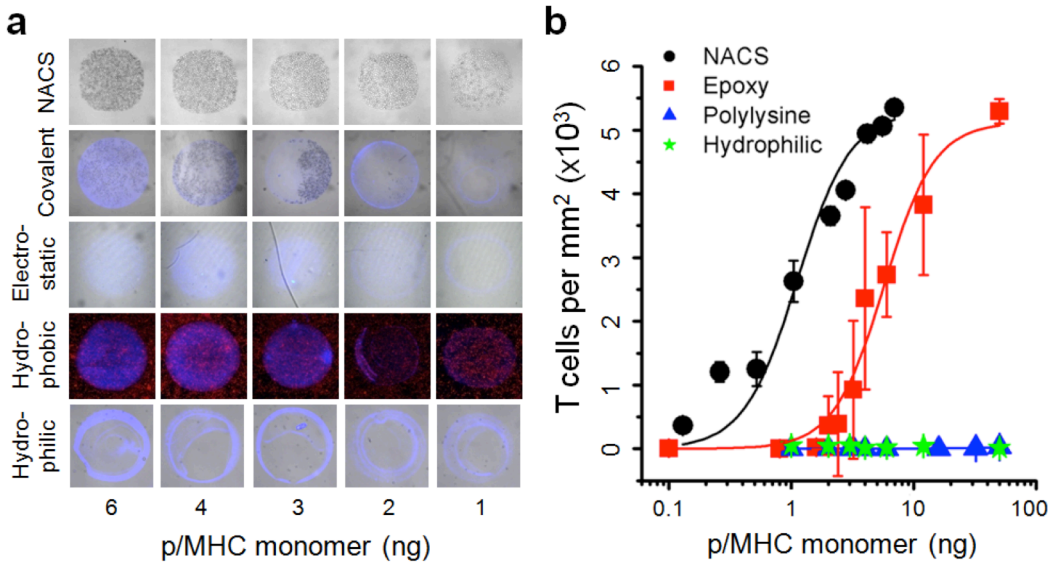

Fig. 2.3. Comparison of NACS versus spotted p/MHC arrays. (**a**) Bright field and fluorescent images of Jurkat$^{a\text{-MART-1}}$ T cell capture on various model substrates. (**b**) Quantification of T cell capture efficiencies (Hydrophobic surface was excluded because signal:noise ≤ 1.)

Compared to conventional microarrays with identical concentration of p/MHC tetramers, NACS was superior. Electrostatic and hydrophilic immobilization have little/no captured T cells, and hydrophobic immobilization has huge noise. Even though covalent immobilization succeeded to capture T cells, it had intra-spot and inter-spot heterogeneity while NACS gave homogeneous result at the same concentration of tetramers. Furthermore, as shown in the quantified analysis, only with a fifth of materials required in covalent immobilization, NACS could capture equivalent T cell. (p/MHC monomer at half max ≡ $K_{1/2}$ = 1.1ng for NACS and 5.7ng for covalent immobilization).

Two factors can be reasons of superior capturing efficiency in NACS. At first, linked by DNA-cDNA hybridization, p/MHC tetramers of NACS have great orientational freedom while those of conventional microarrays hardly have other options except just

absorbed on the surface. This may increase the density of functional p/MHC tetramers and result in reduced $K_{1/2}$. Secondly, NACS does not disrupt hydration state of arrayed proteins, which can be modified during production and storage process of conventional protein microarray to decrease reproducibility[11,16,21]. Because p/MHC tetramer arrays are self-assembled in solution immediately prior to an experiment and only stable DNA oligos are printed on the surface when the chip is stored, NACS may shows intra-spot and inter-spot homogeneity and guarantee the array reproducibility.

2.3.2. Preparation of DNA-encoded antibodies

In the case of protein measurement with SCBC, all the DNA-encoded antibodies should be quantified with BCA kit and calibrated with recombinant proteins before using in on-chip experiment. Their cross-reactivity also must be checked. Without using valves of SCBC, I verified the DNA conjugated antibodies (**Fig. 2.4.a)**, and made calibration curves of each of them with serial dilutions of recombinant solutions (**Fig. 2.4.b**.). The four parameter logistic model is used for fitting the calibration curve, resulting in the fitting parameters in **Table 2.4.**

$$y = \frac{A_1 - A_2}{1 + (x / x_0)^p} + A_2$$

Table 2.4. Parameters utilized for the protein assay calibration curve

	A1		A2		x0		p		Statistics	
	Value	Error	Value	Error	Value	Error	Value	Error	Reduced Chi-Sqr	Adj. R-Square
IL-2	0	0	256	0	7659.58168	973.0838	1.12824	0.16788	91.39131	0.99224
MCP-1	0	0	256	0	65733.51686	4770.5	1.12607	0.09607	29.62623	0.99578
IL-6	0	0	256	0	16231.59942	4515.94	0.67887	0.12265	243.09932	0.95697
GMCSF	0	0	256	0	2451.99685	295.3281	1.2195	0.13013	72.59138	0.99458
MIF	0	0	256	0	7892.74068	483.8218	1.14428	0.07578	20.31714	0.99821
IFN-γ	0	0	256	0	14549.5316	2773.804	1.57222	0.26181	172.2368	0.98713
VEGF	0	0	256	0	1687.9445	225.4782	0.69008	0.05631	58.49911	0.99513
IL-1β	0	0	256	0	2137.44388	208.9672	0.89593	0.07185	41.21361	0.99694
IL-10	0	0	256	0	3961.03661	328.4038	1.23209	0.08611	33.93572	0.99669
IL-8	0	0	256	0	1255.89317	225.9207	1.23262	0.19534	161.8703	0.98686
MMP9	0	0	256	0	70537.40022	1584.696	1.062	0.02495	2.60945	0.99961
TNF-α	0	0	256	0	4126.15703	661.2747	0.81683	0.09483	99.72583	0.99185

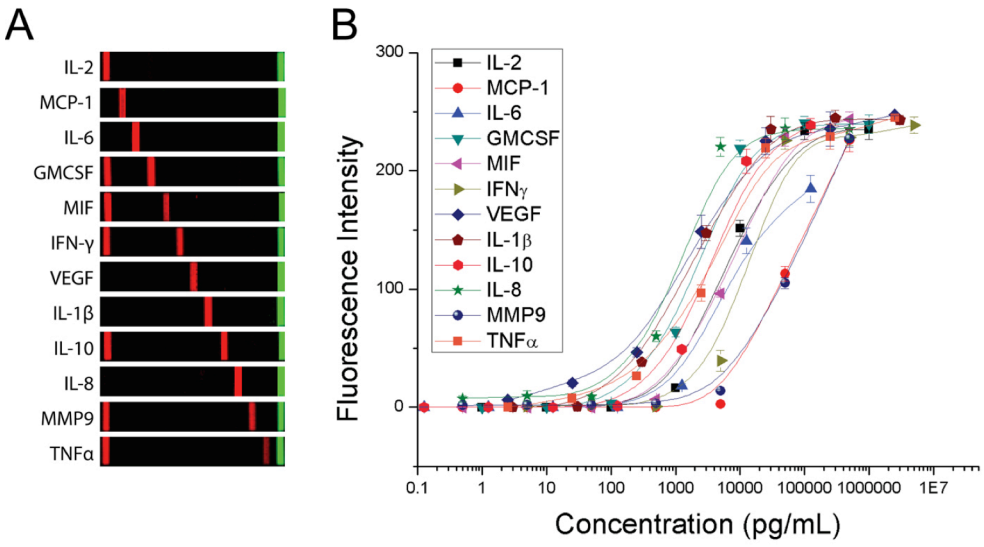

Fig. 2.4. Cross-reactivity check and calibration curves. (A) Scanned image showing cross-reactivity check for all 12 proteins. The green bars represent the reference stripe, sequence M. Each protein can be readily identified by its distance from the reference. In each channel, a standard protein (indicated on the left) was added to the buffer solution and assayed using the DEAL barcode method. For GMCSF, MIF, IFN-γ, IL-10, MMP9, and TNF-α, biotin-labeled 2° anti IL-2 antibody conjugated to DNA sequence A' was used as a control. (B) Quantitation of fluorescence intensity vs. concentration for all 12 proteins. Error bars: 1SD. The variability (defined as the standard deviation divided by the average in percentage) is less than 10% for the signals in detectable range.

2.4. Conclusions

By the comparison with the commercial microarrays, I showed the superiority of NACS platform that can be inexpensively made by traditional DNA printing technologies. Also, I presented the calibration curves of DNA-encoded antibodies, which is essential for the further experiments with SCBC to analyze the protein-protein network in macrophages quantitatively and to predict the role of perturbations.

2.5. References

1. Altman, J. D. *et al.* Phenotypic analysis of antigen-specific T lymphocytes. *Science* **274,** 94–96 (1996).
2. Lamoreaux, L., Roederer, M. & Koup, R. Intracellular cytokine optimization and standard operating procedure. *Nat Protoc* **1,** 1507–1516 (2006).
3. Nomura, L., Maino, V. C. & Maecker, H. T. Standardization and optimization of multiparameter intracellular cytokine staining. *Cytometry A* **73,** 984–991 (2008).
4. Ariztia, E. V., Lee, C. J., Gogoi, R. & Fishman, D. A. The tumor microenvironment: key to early detection. *Crit Rev Clin Lab Sci* **43,** 393–425 (2006).
5. Chen, D. S. *et al.* Marked differences in human melanoma antigen-specific T cell responsiveness after vaccination using a functional microarray. *PLoS Med.* **2,** e265 (2005).
6. Soen, Y., Chen, D. S., Kraft, D. L., Davis, M. M. & Brown, P. O. Detection and characterization of cellular immune responses using peptide-MHC microarrays. *PLoS Biol* **1,** E65 (2003).
7. Stone, J. D., Demkowicz, W. E. & Stern, L. J. HLA-restricted epitope identification and detection of functional T cell responses by using MHC-peptide and costimulatory microarrays. *P Natl Acad Sci USA* **102,** 3744–3749 (2005).
8. Deviren, G., Gupta, K., Paulaitis, M. E. & Schneck, J. P. Detection of antigen-specific T cells on p/MHC microarrays. *J. Mol. Recognit.* **20,** 32–38 (2007).

9. Haab, B. B., Dunham, M. J. & Brown, P. O. Protein microarrays for highly parallel detection and quantitation of specific proteins and antibodies in complex solutions. *Genome Biol.* **2,** RESEARCH0004 (2001).
10. Butler, J. E. *et al.* The physical and functional behavior of capture antibodies adsorbed on polystyrene. *J. Immunol. Methods* **150,** 77–90 (1992).
11. Butler, J. E. *et al.* The immunochemistry of sandwich ELISAs--VI. Greater than 90% of monoclonal and 75% of polyclonal anti-fluorescyl capture antibodies (CAbs) are denatured by passive adsorption. *Mol. Immunol.* **30,** 1165–1175 (1993).
12. MacBeath, G. & Schreiber, S. L. Printing proteins as microarrays for high-throughput function determination. *Science* **289,** 1760–1763 (2000).
13. Lesaicherre, M.-L., Lue, R. Y. P., Chen, G. Y. J., Zhu, Q. & Yao, S. Q. Intein-mediated biotinylation of proteins and its application in a protein microarray. *J. Am. Chem. Soc.* **124,** 8768–8769 (2002).
14. Peluso, P. *et al.* Optimizing antibody immobilization strategies for the construction of protein microarrays. *Anal. Biochem.* **312,** 113–124 (2003).
15. Kwon, Y., Han, Z., Karatan, E., Mrksich, M. & Kay, B. K. Antibody arrays prepared by cutinase-mediated immobilization on self-assembled monolayers. *Anal. Chem.* **76,** 5713–5720 (2004).
16. Arenkov, P. *et al.* Protein microchips: use for immunoassay and enzymatic reactions. *Anal. Biochem.* **278,** 123–131 (2000).
17. Kiyonaka, S. *et al.* Semi-wet peptide/protein array using supramolecular hydrogel. *Nat Mater* **3,** 58–64 (2004).
18. Bailey, R. C., Kwong, G. A., Radu, C. G., Witte, O. N. & Heath, J. R. DNA-encoded antibody libraries: a unified platform for multiplexed cell sorting and detection of genes and proteins. *J. Am. Chem. Soc.* **129,** 1959–1967 (2007).
19. Boozer, C. *et al.* DNA directed protein immobilization on mixed ssDNA/oligo(ethylene glycol) self-assembled monolayers for sensitive biosensors. *Anal. Chem.* **76,** 6967–6972 (2004).
20. Niemeyer, C. M. Functional devices from DNA and proteins. *Nano Today* **2,** 42–52 (2007).

21. Chandra, R. A., Douglas, E. S., Mathies, R. A., Bertozzi, C. R. & Francis, M. B. Programmable cell adhesion encoded by DNA hybridization. *Angew Chem Int Ed Engl* **45,** 896–901 (2006).
22. Fan, R. *et al.* Integrated barcode chips for rapid, multiplexed analysis of proteins in microliter quantities of blood. *Nat Biotechnol* **26,** 1373–1378 (2008).
23. Lin, W.-W. & Karin, M. A cytokine-mediated link between innate immunity, inflammation, and cancer. *J Clin Invest* **117,** 1175–1183 (2007).
24. Gnecchi, M. *et al.* Paracrine action accounts for marked protection of ischemic heart by Akt-modified mesenchymal stem cells. *Nature Publishing Group* **11,** 367–368 (2005).
25. Croci, D. O. *et al.* Dynamic cross-talk between tumor and immune cells in orchestrating the immunosuppressive network at the tumor microenvironment. *Cancer Immunol. Immunother.* **56,** 1687–1700 (2007).
26. Seruga, B., Zhang, H., Bernstein, L. J. & Tannock, I. F. Cytokines and their relationship to the symptoms and outcome of cancer. *Nat Rev Cancer* **8,** 887–899 (2008).
27. Polyak, K. & Weinberg, R. A. Transitions between epithelial and mesenchymal states: acquisition of malignant and stem cell traits. *Nat Rev Cancer* **9,** 265–273 (2009).
28. Sachs, K., Perez, O., Pe'er, D., Lauffenburger, D. A. & Nolan, G. P. CaUSAl protein-signaling networks derived from multiparameter single-cell data. *Science* **308,** 523–529 (2005).
29. Cox, J. H., Ferrari, G. & Janetzki, S. Measurement of cytokine release at the single-cell level using the ELISPOT assay. *Methods* **38,** 274–282 (2006).
30. Song, M. & Phelps, D. S. Comparison of SP-A and LPS effects on the THP-1 monocytic cell line. *Am. J. Physiol. Lung Cell Mol. Physiol.* **279,** L110–7 (2000).
31. SANO, T. & Cantor, C. R. Expression of a cloned streptavidin gene in Escherichia coli. *P Natl Acad Sci USA* **87,** 142–146 (1990).
32. Garboczi, D. N., Hung, D. T. & Wiley, D. C. HLA-A2-peptide complexes: refolding and crystallization of molecules expressed in Escherichia coli and complexed with single antigenic peptides. *P Natl Acad Sci USA* **89,** 3429–3433

(1992).

33. Shin, Y. S. *et al.* Chemistries for patterning robust DNA microbarcodes enable multiplex assays of cytoplasm proteins from single cancer cells. *Chemphyschem* **11,** 3063–3069 (2010).
34. Quake, S. R. & Scherer, A. From micro- to nanofabrication with soft materials. *Science* **290,** 1536–1540 (2000).
35. Millet, L. J., Stewart, M. E., Sweedler, J. V., Nuzzo, R. G. & Gillette, M. U. Microfluidic devices for culturing primary mammalian neurons at low densities. *Lab Chip* **7,** 987–994 (2007).
36. Lee, J. N., Park, C. & Whitesides, G. M. Solvent compatibility of poly(dimethylsiloxane)-based microfluidic devices. *Anal. Chem.* **75,** 6544–6554 (2003).
37. Johnson, L. A. *et al.* Gene transfer of tumor-reactive TCR confers both high avidity and tumor reactivity to nonreactive peripheral blood mononuclear cells and tumor-infiltrating lymphocytes. *J Immunol* **177,** 6548–6559 (2006).